Fission Yeast α-Glucan Synthase Mok1 Requires the Actin Cytoskeleton to Localize the Sites of Growth and Plays an Essential Role in Cell Morphogenesis Downstream of Protein Kinase C Function

Satoshi Katayama,* Dai Hirata,* Manuel Arellano,‡ Pilar Pérez,‡ and Takashi Toda*

*Laboratory of Cell Regulation, Imperial Cancer Research Fund, London WC2A 3PX, United Kingdom, ‡Instituto de Microbiologia Bioquimica, CSIC/Universidad de Salamanca, Edificio Departamental, 37007 Salamanca, Spain

Abstract. In fission yeast protein kinase C homologues (Pck1 and Pck2) are essential for cell morphogenesis. We have isolated *mok1*$^+$ in a genetic screen to identify downstream effectors for Pck1/2. *mok1*$^+$ is essential for viability and encodes a protein that has several membrane-spanning domains and regions homologous to glucan metabolic enzymes. *mok1* mutant shows abnormal cell shape, randomization of F-actin and weak cell wall. Biochemical analysis shows that Mok1 appears to have α-glucan synthase activity. Mok1 localization undergoes dramatic alteration during the cell cycle. It localizes to the growing tips in interphase, the medial ring upon mitosis, a double ring before and dense dot during cytokinesis. Double immunofluorescence staining shows that Mok1 exists in close proximity to actin. The subcellular localization of Mok1 is dependent upon the integrity of the F-actin cytoskeleton. Conversely, overexpression of *mok1*$^+$ blocks the translocation of cortical actin from one end of the cell to the other. *pck2* mutant is synthetically lethal with *mok1* mutant, delocalizes Mok1 and shows a lower level of α-glucan. These results indicate that Mok1 plays a crucial role in cell morphogenesis interdependently of the actin cytoskeleton and works as one of downstream effectors for Pck1/2.

Key words: actin • α-glucan synthase • fission yeast • morphogenesis • protein kinase C

Cell morphogenesis is of fundamental importance for all eukaryotic cells. Both the budding yeast *Saccharomyces cerevisiae* and fission yeast *Schizosaccharomyces pombe*, have been extensively used as model systems to study the basic questions of cell morphogenesis (Nurse, 1994; Drubin and Nelson, 1996). Unlike animal cells but in common with plant cells, yeast cells have a rigid cell wall that is composed of extracellular polysaccharides, mostly glucan, and interstitial component glycoproteins (Cabib et al., 1997). The application of the term rigid in terms of cell wall architecture by no means implies that cell wall architecture or composition is a static matrix unchanged in any condition. In fact, the cell wall is a highly dynamic structure, the architecture and composition of which are coordinately regulated with cell growth. For example, at the specific growing sites such as elongating tips or budding sites, two opposing reactions, degradation and synthesis of cell wall components, simultaneously occur in a concerted manner to generate polarized growth (Cabib et al., 1997). Upon cell division, the actomyosin system forms a contractile ring-like structure, which is essential for cytokinesis and directs the coordinated formation of the septum. Upon sexual differentiation, the cell wall is reorganized to enable fusion of two cells of opposite mating types.

Recent advances have shed light on the importance of the cell wall as a crucial apparatus through which information of extracellular cues is transmitted and integrated into intracellular processes. The best example is the close relationship between the activity of a ubiquitous small GTP-binding protein Rho1 and 1,3-β-D-glucan synthase. 1,3-β-D-glucan is responsible for the synthesis of a major component of the cell wall and in budding yeast and most probably also in fission yeast, Rho1 is a regulatory component of 1,3-β-D-glucan synthase holoenzymes (Arellano et al., 1996; Drgonová et al., 1996; Qadota et al., 1996). In higher eukaryotes, RHO GTPases have also been shown

Address correspondence to Takashi Toda, Laboratory of Cell Regulation, Imperial Cancer Research Fund, PO Box 123, 44 Lincoln's Inn Fields, London WC2A 3PX, UK. Tel.: 44 171 269 3535. Fax: 44-171-269-3258. E-mail: toda@europa.lif.icnet.uk

Dr. Hirata's present address is Department of Molecular Biotechnology, Graduate School of Advanced Sciences of Matter, Hiroshima University, and "Unit Process and Combined Circuit," PRESTO, JST, Higashi-Hiroshima 739-8526, Japan.

Published March 22, 1999

to be crucial regulators of cell morphogenesis, especially in the regulation of the organization of the actin cytoskeleton (Hall, 1998). A number of RHO effectors have been identified in both animals and yeasts (Ridley, 1996; Tanaka and Takai, 1998). In yeasts, in addition to 1,3-β-D-glucan synthase, protein kinase C (PKC)[1]-related molecules are Rho1 effectors (Nonaka et al., 1995; Toda, 1997). In this context, it is of particular significance that in mammalian cells, PKC-related protein kinases PRK/PKN are also downstream effectors for RHO (Amano et al., 1996; Watanabe et al., 1996; Flynn et al., 1998). Both cell morphology and cell wall integrity are impaired in mutants defective in yeast PKC function (Levin and Bartrett-Heubusch, 1992; Toda et al., 1993), again highlighting the importance of the cell wall biogenesis in yeasts as a model for understanding signal transduction pathways involving RHO and PKC-related molecules.

Despite collectively being called yeasts, the cell shapes of budding and fission yeasts are very different; budding yeast is oval, whereas fission yeast is cylindrical. In addition and not surprisingly, the cell wall compositions of these two yeasts differ. The major components of cell wall polysaccharides in budding yeast are 1,3-β-D-glucan, 1,6-β-D-glucan and chitin (Cabib et al., 1997). On the other hand, in fission yeast, β-glucan and 1,3-α-D-glucan are the major components (Manners and Meyer, 1977; Kopecká et al., 1995). In contrast to studies on the biogenesis of β-glucan, our understanding of the biogenesis of α-glucan is limited (Ishiguro et al., 1997; Ishiguro, 1998). It is, nonetheless, inferred that this polysaccharide plays an essential role in the maintenance of cell shape and polarity control as the treatment of α-glucanase results in complete remodeling of the rod-shaped cells into round protoplasts, whereas treatment with β-glucanase leaves cells morphologically unaffected (Moreno et al., 1991). It is, therefore, crucial to know how 1,3-α-D-glucan is synthesized and how its synthesis is regulated during the cell cycle and developmental processes.

We have previously shown that fission yeast PKC-related protein kinases Pck1 and Pck2 play essential roles in maintaining cell viability and cell integrity. They are required to maintain proper cell shape and cell wall structures (Toda et al., 1993; Kobori et al., 1994). We have also shown that, as in budding yeast, Pck1 and Pck2 are downstream targets for Rho1 (Sayers, L., K. Nakano, I. Mabuchi, S. Katayama, T. Toda, and P. Parker, unpublished results). Previous work has identified both the Pmk1-MAP kinase and Sts5 as proteins functionally interacting with Pck1 and Pck2 to regulate cell integrity (Toda et al., 1996a,b). Despite this effort, effector molecules that act downstream of Pck1 and Pck2 to directly regulate cell shape and cell wall integrity await identification.

To explore the molecular pathways by which Pck1 and Pck2 regulate cell integrity, a novel large scale screen for potential downstream targets has been undertaken. Mutations in the novel gene, *mok1*$^+$ (see below) result in defects in cell morphogenesis as well as in the function of Pck1 and Pck2. We show that the Mok1 protein is most probably the α-glucan synthase. Surprisingly the fission yeast genome contains a *mok1*$^+$-related gene family, comprising at least five members. The Mok1 protein plays a vital role in cell morphogenesis and localizes in close proximity to the actin cytoskeleton throughout the mitotic cell cycle. Possible functions of Mok1 in cell morphogenesis in relation to Pck1 and Pck2 are discussed.

Materials and Methods

Strains, Media, and Chemicals

Strains used in this study are listed in Table I. Complete medium, YPD (1% yeast extract, 2% polypeptone, 2% dextrose) which contains 10 μg/ml Phloxine B (called YPDP), YES5 (0.5% yeast extract, 3% dextrose, and 75 μg/ml of adenine, histidine, leucine, and uracil), and modified synthetic EMM2 have been described (Moreno et al., 1991).

Genetic Techniques and Nomenclature

Standard procedures for *S. pombe* genetics were followed according to Moreno et al. (1991). Gene disruptions are abbreviated by putting the symbol Δ before the gene name, e.g., Δ*mok1*. Proteins are designated by an uppercase first letter, e.g., Mok1.

Isolation of Conditional Lethal Mutants with Morphological Defects

As an initial screen collection of temperature-sensitive (ts) or cold-sensitive (cs) mutants (2,822 or 1,961, the restrictive temperatures were set at 36 and 20°C, respectively) were visually selected by calcofluor staining and morphological mutants with altered cell shape at the restrictive temperature were isolated. Four types of morphological mutants were observed, namely round or pear-like, elongated, bent or branched, and septation defective. Round or pear-shaped mutants were further screened for the supersensitivity to a protein kinase inhibitor staurosporine (STS, 1.5 μg/ml) for which Pck1 and Pck2 are two of the major targets (Toda et al., 1993). To exclude mutants that were nonspecifically supersensitive to a broad range of drugs, sensitivity to K-252a (3 μg/ml), which structurally related but has distinct biological targets to STS (Tamaoki and Nakano, 1990), was also examined.

Table I. Strain List

Strains	Genotypes	Deviations
HM123	*h*$^-$*leu1*	Our stock
DH664	*h*$^-$*leu1mok1-664*	This study
PN18	*h*$^-$*cdc3-6*	From P. Nurse (Imperial Cancer Research Fund, London, UK)
PN100	*h*$^-$*cdc8-27*	From P. Nurse
SKDP1	*h*$^-$/*h*$^+$*leu1/leu1ura4/ura4his7/his7 ade6-M210/ade6-M216mok1::ura4*$^+$/+	This study
SKP11	*h*$^-$*leu1ura4his7ade6mok11::ura4*$^+$	This study
SKP12	*h*$^-$*leu1ura4his7ade6mok12::ura4*$^+$	This study
SKP13	*h*$^-$*leu1ura4his7ade6mok13::ura4*$^+$	This study
SKP1112	*h*$^-$*leu1ura4his7ade6mok11::ura4mok12::ura4*$^+$	This study
SKP1124	*h*$^-$*leu1ura4his7ade6mok11::ura4mok12::ura4*$^+$*mok14::kan*	This study
SKP103	*h*$^-$*leu1nmt1-mok1*$^+$*-kan*	This study
TP170-2B	*h*$^-$*leu1pck2::LEU2*	Toda et al., 1993
TP134-3B	*h*$^-$*leu1ura4pck1::ura4*$^+$	Toda et al., 1993
SKP170	*h*$^-$*leu1pck2::LEU2nmt1-mok1*$^+$*-kan*	This study
SKP100	*h*$^-$*leu1mok1-664pck2::LEU2*	This study
SKP101	*h*$^-$*leu1ura4mok1-664pck1::ura4*$^+$	This study

1. *Abbreviations used in this paper:* cs, cold-sensitive; GFP, green fluorescent protein; HA, hemagglutinin; lat A, latrunculin A; PKC, protein kinase C; STS, staurosporine; ts, temperature-sensitive.

Published March 22, 1999

Complementation Tests

After mating of each strain, free spores were directly plated on four YPDP plates, three of which were incubated at 20, 29, or 36°C and the fourth was incubated on a YPDP plate containing 1.5 μg/ml STS at 29°C. If the difference in colony number between the plates growing under these conditions was $>10^4$-fold, the two mutants were assumed to be allelic.

Nucleic Acids Preparation and Manipulation

Standard molecular biology techniques were followed as described (Sambrook et al., 1989). Enzymes were used according to the recommendation of the suppliers (New England Biolabs Inc.). Nucleotide sequence was determined by use of dideoxy-method (Sanger et al., 1977).

Cloning of the *mok1*$^+$ Gene

An *S. pombe* genomic library constructed in the vector pDB248 (Moreno et al., 1991) was used for the isolation of plasmids that complemented the ts *mok1* mutant (DH664). 2 out of 20,000 colonies were capable of growing at 36°C and the segregation analysis showed that the Ts$^+$ phenotype was plasmid-dependent. Two different plasmids (pMK100 and pMK1100) containing different, but overlapping, inserts were isolated. Subcloning analysis indicated that the internal SmaI site was essential for the complementing activity of pMK1100. When the 5.5-kb SmaI/BamHI fragment was subcloned from pMK1100, the resulting plasmid (pMK1101) lost the complementing activity. However, Ts$^+$ colonies appeared from transformants containing pMK1101 at a frequency of $\sim 10^{-3}$. It was found that pMK1101 directed integration of the *LEU2* marker into the genome via homologous recombination in these Ts$^+$ transformants. Subsequent analysis showed that no ts recombinants arose from 10^4 recombinants between this integrant and a wild-type strain. This result demonstrated that pMK1101 contains the *mok1*$^+$ gene itself.

Identification of *mok1*$^+$-related Genes in the Fission Yeast Genome

Homology searching using Mok1 as query against the fission yeast genome database (Sanger Centre, Cambridge, UK) showed that there are four additional *mok1*$^+$ homologues [designated *mok11*$^+$ (SPAC23D3), *mok12*$^+$ (SPAB4538), *mok13*$^+$ (c16D10S), and *mok14*$^+$ (c63), respectively]. The nucleotide sequence data reported in this paper will appear in the DDBJ/EMBL/Genbank nucleotide sequence databases under the accession numbers: AB019183 (*mok1*$^+$), AB018380 (*mok11*$^+$), AB018381 (*mok12*$^+$), AB018382 (*mok13*$^+$), and AB018383 (*mok14*$^+$).

Gene Disruption of *mok1*$^+$, *mok11*$^+$, *mok12*$^+$, *mok13*$^+$, and *mok14*$^+$

Three different strategies were taken to disrupt the *mok1*$^+$ gene by use of a PCR-generated fragment containing the *ura4*$^+$ marker (Bähler et al., 1998): one resulted in the complete deletion of the ORF (SKDP1), the second in deletion of a 1,764 bp NH_2-terminal fragment (corresponding to amino acids 66–654) and the third in fusing the DNA encoding HA or GFP tags to the COOH terminus, which was accidentally found during the attempt to construct the tagged *mok1*$^+$ gene. Correct disruption was verified by PCR. In both cases, tetrad analysis of the heterozygous diploid showed two viable (Ura$^-$) and two inviable spores, indicating that the *mok1*$^+$ gene is essential for cell viability. The *mok11*$^+$, *mok12*$^+$, *mok13*$^+$, and *mok14*$^+$ genes were also disrupted. Tetrad analysis of a heterozygous diploid yielded four viable spores, in which Ura$^+$ and Ura$^-$ segregates 2:2 in each case. This indicated that neither *mok11*$^+$, *mok12*$^+$, nor *mok13*$^+$ gene is essential for cell viability. It was also found that double *mok11mok12* and triple *mok11mok12mok14* disruptions were viable.

Overexpression of the *mok1*$^+$ Gene

Three different fragments of the *mok1*$^+$ gene were amplified with PCR and inserted in pREP1 or pREP2 (the *nmt1* promoter-containing vector; Maundrell, 1990); a 7.2-kb fragment containing the whole ORF (5′-TTTGGATCCTATGCATGGTCTTCAAGGGTTATGTTTTAGA-3′ and 5′-TTTGGATCCCTAAGGACGACTAAGGTTTTCACGACGGAA-3′ were used for PCR, yielding pREP1-mok1), an NH_2-terminal 3.4 kb containing amino acid residues 1–1,236 (5′-TTTAGGCCTCTACGAGACTACAGGAGTGACCTT-3′ and 5′-TTTGGATCCTATGCATGGTCTTCAAGGGTTATGTTTTAGA-3′ were used for PCR, yielding pREP2-mok1N) and a COOH-terminal 3.9 kb containing amino acid residues 1,017 to 2,410 (5′-TTTGGATCCTATGCATGGTCTTCAAGGGTTATGTTTTAGA-3′ and 5′-TTTGGATCCCTAAGGACGACTAAGGTTTTCACGACGGAA-3′ were used for PCR, yielding pREP1-mok1C). The *nmt1* promoter was integrated in the genome in front of the initiator ATG of the *mok1*$^+$ gene by a PCR-based gene targeting method (SKP103; Bähler et al., 1998).

Time-lapse Microscopy

Fission yeast cells, in which the *nmt1* promoter was integrated in front of the ORF of *mok1*$^+$ (SKP103), were grown in liquid minimal medium at 29°C for 12 h and placed on a slide glass embedded in a slice (1 mm) of agar made of minimal medium supplemented with leucine. This slice was then overlaid with a coverslip and sealed with liquid sealer. The slide glass was set under the phase microscope (Zeiss Co.) at room temperature (22°C) and the cells were viewed with a chilled video-rated CCD camera (model C5985; Hamamatsu) connected to a computer (Apple Power Macintosh 8600/200). Photographs of live cells in a fixed field were taken every 30 min. Images were processed by use of Adobe® Photoshop (version 4).

Fractionation and Labeling of Cell Wall Polysaccharides

Cultures of *S. pombe* cells were supplemented with U-[^{14}C]glucose (1 μCi/ml) and incubated for additional 4 h. To label cells overproducing *mok1*$^+$ (SKP103 and SKP170), cultures were induced for 14 h in the absence of thiamine before addition of U-[^{14}C]glucose. Total glucose incorporation was monitored by measuring the radioactivity in trichloroacetic acid insoluble material. Mechanical breakage of cells was done as described (Arellano et al., 1996, 1997) and cell walls were pelleted at 1,000 *g* for 5 min. 100 μl aliquots of the total wall were incubated with 100 units of zymolyase 100T (Seikagaku Kogyo Co. Ltd.) or Quantazyme (Quantum Biotechnologies Inc.) for 36 h at 30°C. The samples were centrifuged and the supernatant and washed pellet were counted separately. The polysaccharides in the supernatant from the zymolyase 100T reaction were considered to be β-glucan plus galactomannan, and the pellet α-glucan, whereas that from the Quantazyme reactions was considered to be β-glucan and the pellet α-glucan plus galactomannan.

Immunological Assays

Rabbit polyclonal anti-Mok1 antibody was prepared as follows. To express the fused Mok1 protein, the 0.9-kb fragment corresponding amino acid residues 1,583 to 1,904 (5′-TTTCATATGTCTCAACGTACCCGTGCTCGACTT-3′ and 5′-TTTGGATCCATCTCTGATTTCATTAAGTATTGT-3′ were used for PCR) was inserted into pET10c (Invitrogen Co.). Insoluble proteins were purified using Ni-NTA column. Two rabbits were injected with the Mok1 fusion protein (200 μg per injection). Immunoblotting was performed with crude sera or affinity-purified anti-Mok1 antibodies. Bacterially made Mok1 fusion protein was bound to nitrocellulose filters in order to purify anti-Mok1 antibodies from crude sera. Monoclonal anti–α-tubulin antibody (Sigma Chemical Co.) was also used. Horseradish peroxidase-conjugated goat anti–rabbit IgG, goat anti–mouse IgG (Bio-Rad Laboratories Ltd.) and a chemiluminescence system (ECL; Amersham Corp.) were used to detect bound antibody.

Fission yeast whole cell extracts were prepared using glass beads to disrupt yeast cells in TEG buffer (50 mM Tris-HCl, pH 7.5, 1 mM EDTA, 10% glycerol, 30 mM NaCl, 1 mM DTT, 60 mM β-glycerophosphate, 15 mM *p*-nitrophenylphosphate, 0.1 mM NaF, 10 μg/ml soybean trypsin inhibitor, 20 μg/ml leupeptin, 50 μg/ml aprotinin, 2 μg/ml pepstatin, 1 mM PMSF, and 0.1 mM Na-orthovanadate). For the subcellular fractionation, cell extracts were microcentrifuged at 13,000 rpm for 15 min at 4°C in various conditions in order to separate soluble from insoluble fractions.

Indirect Immunofluorescence Microscopy

Rhodamine-conjugated phalloidin (Molecular Probes Inc.) or monoclonal anti-chicken gizzard actin antibody (N-350; Amersham Corp.) followed by Cy3-conjugated sheep anti–mouse IgG (Sigma Chemical Co.) was used to visualize actin as described previously (Toda et al., 1996b). Rabbit polyclonal anti-Mok1 serum (1:10 dilution) or undiluted affinity-purified anti-

Published March 22, 1999

bodies and Cy3-conjugated goat anti–rabbit IgG (Sigma Chemical Co.) or FITC-conjugated swine anti–rabbit IgG (DAKO Ltd.) was used to localize the Mok1 protein.

Treatment with Latrunculin A

A stock solution of latrunculin A (lat A; Molecular Probes Inc.) was made in DMSO (50 mM) and used at a concentration of 100 μM. DMSO alone did not affect the F-actin cytoskeleton or Mok1 distribution.

nmt1 Promoter Shut-off

Cells containing *nmt1-mok1*$^+$ (SP103) grown at 29°C in minimal medium in the presence of 5 μM thiamine were filtered, resuspended in minimal medium without thiamine, and incubated for further 12 h to induce the *nmt1* promoter. Then thiamine (5 μM) and cycloheximide (100 μg/ml) were added, cell extracts prepared every 15 min and immunoblotted with anti-Mok1 antibody.

Results

Isolation of Morphological Mutants that Are Impaired in Protein Kinase C Function

A genetic screen was performed in order to identify genes that regulate cell morphogenesis and function in the protein kinase C (PKC) pathway. Mutants that showed round or pear-shaped morphology at the restrictive temperature were visually isolated from a collection of ts or cs mutants. We have previously shown that two of the major targets of a protein kinase inhibitor staurosporine (STS) in fission yeast are PKC-related molecules, Pck1 and Pck2 (Toda et al., 1993), and that mutants defective in Pck1 and Pck2 function are supersensitive to this drug (Toda et al., 1996b). Accordingly, the sensitivity of each round or pear-like mutant to STS was examined. In total 25 ts and 6 cs mutants were identified that satisfied both criteria. These loci were designated *mok* (morphological and kinase-inhibitor supersensitive).

Complementation analysis of these *mok* mutants and known morphological mutants showed that they defined 10 different loci (*mok1-10*, Table II). *mok2* (eight alleles) and *mok3* (one allele) were allelic to *sts5/orb4* and *pck2/sts6*, respectively, which have previously been shown to produce STS-supersensitive round mutants (Toda et al., 1993, 1996b). The most frequently isolated locus was *mok1* (twelve ts and two cs alleles, Table II).

Table II. Complementation Groups of the mok Mutants

Loci	No. of alleles*	Growth	Morphology	Allelic to:	Gene products
mok1	14	ts or cs	Round	*ags1*‡	α-Glucan synthase
mok2	8		Round	*sts5/orb4*§	Homology to RNase II
mok3	1		Pear-shaped	*pck2/sts6*‖	PKC-like
mok4	1	ts	Pear-shaped		
mok5	1	ts	Pear-shaped		
mok6	1		Pear-shaped		
mok7	1		Pear-shaped		
mok8	1	cs	Pear-shaped		
mok9	1	cs	Pear-shaped		
mok10	2		Round		

*The allele numbers of each *mok* mutant are the following: *mok1-559, -664, -905, -907, -936, -1071, -1172, -1221, -1224, -1489, -1944, -1963* (12 ts alleles), *c624, c706* (2 cs alleles); *mok2-171, -276, -371, -563, -572, -1021, -1537, -1698*; *mok3-24*; *mok4-1572*; *mok5-1747*; *mok6-1698*; *mok7-1787*; *mok8-c68*; *mok9-c188*; *mok10-c214, -c727*.
‡Hochstenbach et al., 1998
§Toda et al., 1996b
‖Toda et al., 1993

Defective Cortical F-Actin Localization and Cell Wall Integrity in mok1 Mutants

The localization of F-actin was examined to characterize the defective phenotypes of *mok1* mutants. In fission yeast F-actin localizes to either the growing tips or the medial regions of dividing cells where the septum forms (Marks and Hyams, 1985; Marks et al., 1986, see Fig. 1 a, left). In contrast to wild-type patterns, cortical actin did not show the specific localization in the *mok1-664* mutant incubated

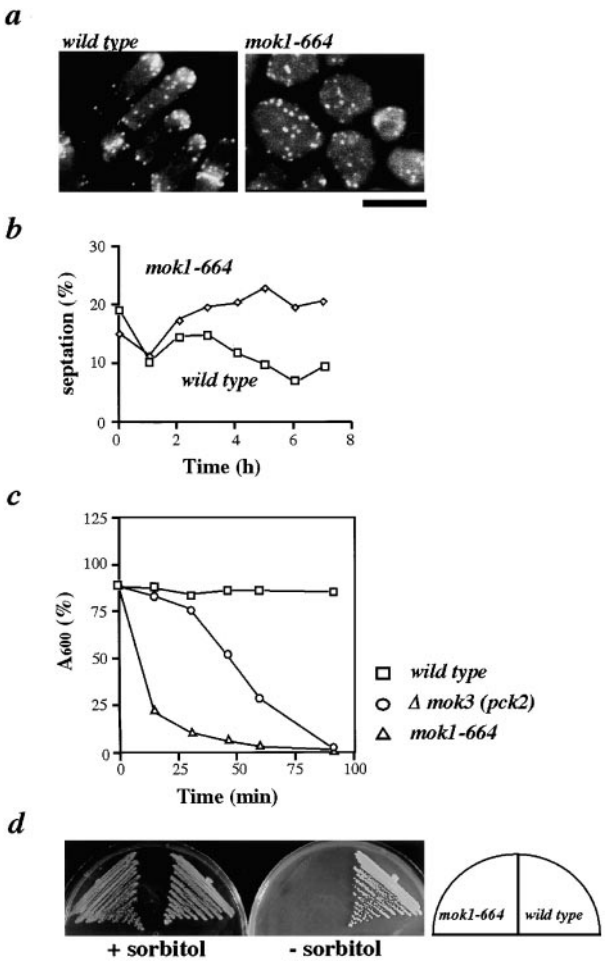

Figure 1. The *mok1* mutants are defective in cell shape, F-actin localization, cytokinesis and cell wall integrity. (a) Localization of F-actin in *mok1* mutants. Wild-type (left, HM123) and the ts *mok1-664* mutant cells (right, DH664) were incubated at 35.5°C for 6 h, fixed and stained with rhodamine-conjugated phalloidin. The bar indicates 10 μm. (b) Percentage of septated cells. Wild-type and *mok1-664* strains were incubated at 35.5°C and septation index measured hourly with calcofluor staining. (c) Defects in cell wall integrity. Wild-type, Δ*pck2* (TP170-2B) and ts *mok1* mutant cells were grown at 28°C and treated with 100 μg/ml of zymolyase (Seikagaku Kogyo). Cell lysis was monitored by measuring optical density (OD_{600}). (d) Rescue of the *mok1* mutants with high osmolarity. Wild-type and *mok1* mutant cells were streaked on a rich YPD plate (right) or that containing 1.2 M sorbitol (left) and incubated at 35.5°C for 3 d.

Published March 22, 1999

at 35.5°C for 6 h. Instead, it localized in the cell cortex in a random punctate (right). Percentage of septated cells slightly increased at the restrictive temperature (19% at 26°C and 22% at 36°C for 6 h, Fig. 1 b), suggesting that *mok1* mutant is also defective in cell separation. The *mok1*$^+$ gene is, therefore, required for the maintenance of rod-shape, cytokinesis and the cellular localization of F-actin.

pck2 mutants are defective in cell wall integrity and, as a result, these cells are supersensitive to treatment with cell wall digesting enzymes (Shiozaki and Russell, 1995; Toda et al., 1996a,b). To determine the morphology defect of *mok1* mutants was also due to an inability to maintain cell wall integrity, mutant cells were treated with β-glucanase. Like *pck2*, the *mok1* mutants were hypersensitive to β-glucanase even at the temperature permissive of 28°C (Fig. 1 c). Defects in cell wall integrity can be sometimes compensated for by increases in the osmolarity of the growth media (Levin and Bartrett-Heubusch, 1992). Consistently *mok1* mutant cells were capable of forming colonies at 35.5°C on rich YPD plates containing 1.2 M sorbitol (Fig. 1 d). Also the *mok1* mutants were hypersensitive to calcofluor, which disrupts cell wall architecture (data not shown). Therefore, the ts and morphological defective phenotypes of *mok1* mutants were, at least in part, ascribable to defects in cell wall integrity.

The Predicted mok1$^+$ *Gene Product Encodes a Large Protein with Multiple Transmembrane Domains and Homology to Enzymes Involved in Glucan Metabolism*

The *mok1*$^+$ gene was cloned by complementation of the ts defect. Nucleotide sequencing of the cloned DNA fragment identified an uninterrupted ORF consisting of 7,230 bp which encoded a protein of 2,410 amino acid residues (the predicted molecular mass is 272 kD). Homology searching and structural analysis showed that the Mok1 protein comprises five structural domains (Fig. 2, a and b). The first is the NH_2-terminal 30 amino acid residues, which are highly hydrophobic and probably act as a signal peptide. The second domain follows the first 1,000 amino acid residues and has three transmembrane domains. A significant homology to a group of glycoside hydrolases, including bacterial α-amylase (Henrissat and Davies, 1997) was found within this region (Fig. 2 b). The third domain is a central, putative transmembrane, domain (amino acid residues 1,070–1,090). The fourth comprises the next 1,000 amino acid residues which show significant homology to both bacterial glycogen synthase (Kumar et al., 1986) and plant starch synthase (van der Leij et al., 1991; Fig. 2 b). Consistent with the homology between Mok1 and glucan synthases, two consensus sequences for UDP-glucose binding motifs (Furukawa et al., 1993) were found in Mok1 (Fig. 2 c). Mok1 and plant starch synthase further share a similarity in the N-terminal signal peptide and the region after the amylase-homologous region (Fig. 2 b). The fifth domain is the COOH-terminal 400 amino acid residues that predict 12 membrane spanning domains (Fig. 2 a). Thus the predicted structure suggests that Mok1 is an integral membrane protein that plays a role in degradation or synthesis of cell wall components.

Homology searching against the fission yeast genome

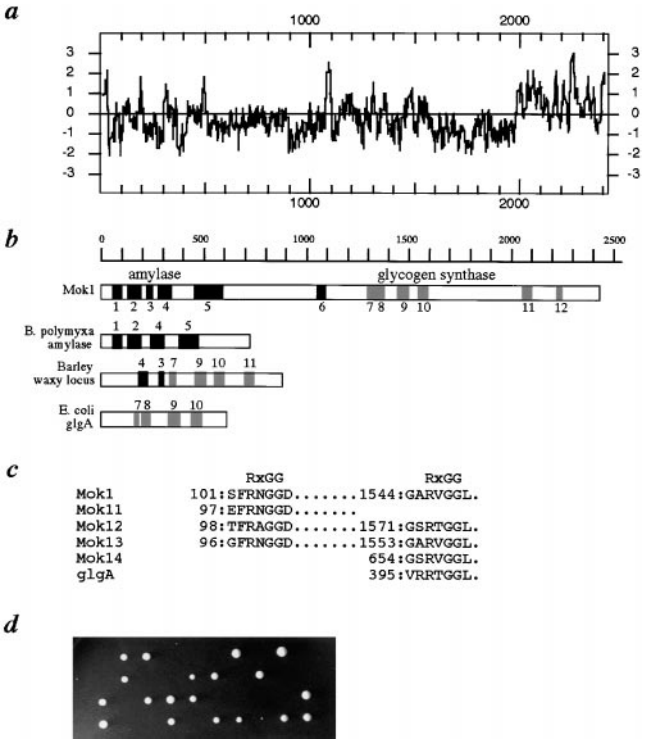

Figure 2. The *mok1*$^+$ gene encodes an essential putative membrane protein with homology to glucan metabolic enzymes. (a) Hydophobicity profile of Mok1. Hydropathy plot is performed according to Kyte and Doolittle (1982). (b) A schematic presentation of homology between Mok1 and various glucan metabolic enzymes. These include bacterial α-amylase (the homologous regions are shown with closed boxes with numbers), plant starch synthase (waxy, the homologous regions are shown with shaded boxes with numbers) and bacterial glycogen synthase (glgA). The central transmembrane domain is also marked (numbered 6). (c) Comparison of a consensus sequence for UDP-glucose binding. (d) Tetrad analysis of a heterozygous diploid. Diploid (SKDP1) which consisted of one copy of wild-type *mok1*$^+$ and its complete deletion allele was manipulated and incubated on YPD plate at 30°C for 3 d.

database (Sanger Centre) indicated that *mok1*$^+$ constitutes a gene family; four putative homologues (designated *mok11*$^+$, *mok12*$^+$, *mok13*$^+$, and *mok14*$^+$) are found in the genome sequences that are currently available. The predicted *mok11*$^+$ (COOH terminus is unsequenced), *mok12*$^+$ and *mok13*$^+$ gene products also encode larger proteins (1,204, 2,352, and 2,371 amino acid residues, respectively), whereas *mok14*$^+$ encodes a smaller protein (1,369 amino acid residues) which lacks the NH_2-terminal amylase-homologous region. The overall homology among these proteins is 40–50% identity (50–60% similarity; Table III) and all of them share virtually identical hydrophobicity profiles. It is of note that budding yeast does not contain any proteins that share significant homology to Mok1.

Characterization of the Mutation Sites in the mok1 Mutants

Different *mok1* mutants alleles (*mok1-559, -664, -905, -936, -1071, -1172, -1221, -1224,* and *-1963*) were transformed with the noncomplementing plasmid pMK1101 (containing amino acid residues 1–876) and transformants were

Published March 22, 1999

Table III. Similarity between Mok1 and Other Members of the Protein Family

	Mok1	Mok11	Mok12	Mok13
Mok11	49 (62)			
Mok12	39 (51)	38 (52)		
Mok13	48 (60)	48 (61)	38 (52)	
Mok14	40 (50)	NA	37 (50)	42 (55)

Percentage of identity and similarity (parentheses) of the amino acid sequence among each pair of proteins is shown. NA, not applicable.

streaked and incubated at 35.5°C. In all nine ts *mok1* mutant alleles tested, Ts^+ integrants appeared at a frequency of $\sim 10^{-3}$. Thus, the mutation sites in these *mok1* mutants are in the region of the NH_2-terminal 876 amino acid residues.

The mok1$^+$ Gene Is Essential for Cell Viability

The *mok1*$^+$ gene was disrupted by three different strategies (Materials and Methods). In each case, tetrad analysis indicated that two viable and two inviable spores were obtained (Fig. 2 d) and that viable spores produced Ura^- colonies. Microscopic observation of inviable spores showed that most of the Δ*mok1* spores (18 out of 20 spores) failed to germinate. Therefore, *mok1*$^+$ is essential for cell viability and also is required for germination.

Ectopic Overexpression of mok1$^+$ Is Lethal and Results in Defects in Cell Shape, the Localization of F-Actin, and Deposition of Cell Wall Material

To examine phenotypes arising from overexpression of *mok1*$^+$, three different plasmids, which contained the whole ORF, the NH_2-terminal 1,236 amino acid residues, and the COOH-terminal 1,393 amino acid residues respectively, were constructed in a vector carrying the thiamine-repressible *nmt1* promoter (Fig. 3 a). In addition, the *nmt1* promoter was integrated into the genome in front of the *mok1*$^+$ gene initiator methionine (ATG). It was found that overexpression of the entire *mok1*$^+$ gene (*nmt-mok1*$^+$), either episomal or integrated, was toxic (Fig. 3 b). Viability dropped sharply upon induction of the *nmt1* promoter (25 and 15% after 14 and 18 h induction, respectively, Fig. 3 c). In contrast, overexpression of the NH_2-terminal or COOH-terminal half did not affect viability (Fig. 3 a).

Cell morphology after induction of *nmt1-mok1*$^+$ was examined. Two types of cell shape defects were found. One showed an asymmetrical shape in which one end of the cell swelled abnormally to produce a tadpole (Fig. 3 d, 62% after 20 h induction). The other was observed as pairs of divided cells associated side-by-side (12%), the cell wall of which appeared fragile and often lysed upon division.

To examine the deposition of cell wall material and the localization of actin in *mok1*$^+$-overexpressing cells, cells

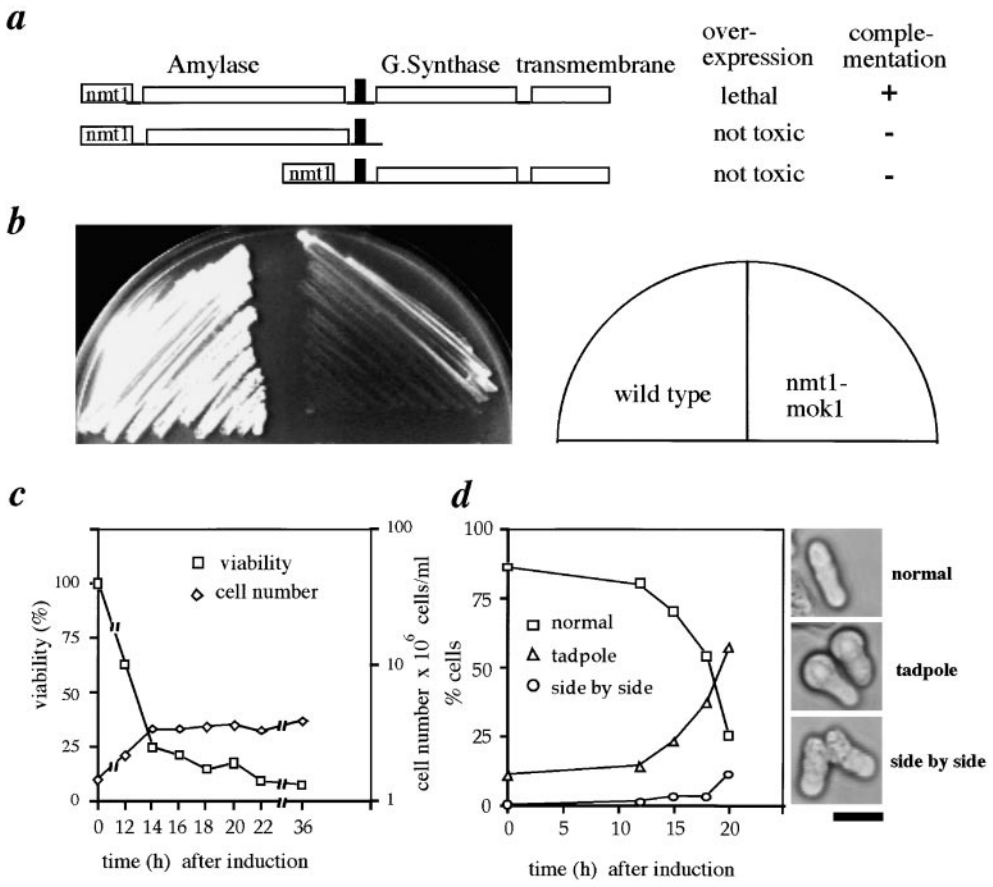

Figure 3. Ectopic overexpression of *mok1*$^+$ is lethal. (a) Three different constructs to direct overexpression of different portions of *mok1*$^+$. The whole ORF (top), the NH_2-terminal half (middle), and the COOH-terminal half (bottom) were inserted into a vector carrying the *nmt1* promoter. (b) Toxicity of overexpression of the *mok1*$^+$ gene. Wild-type cells containing an empty vector (pREP) or a plasmid carrying *nmt-mok1*$^+$ were streaked on the minimal plates in the absence of thiamine (derepressed) and incubated at 29°C for 3 d. (c) Viability upon *mok1*$^+$ overexpression. Cell number and relative viability of cells in which expression of genomic *mok1*$^+$ was regulated by the *nmt1* promoter (SKP103) are shown. At time 0, thiamine was removed from the medium. Cell viability at time 0 was calculated as 100% (viability: the number of colonies divided by the cell number was 88% at time 0). (*d*) Abnormal cell morphology by *mok1*$^+$ overexpression. The frequency of individual cell types are shown. These are: cylindrical (normal), tadpole and side-by-side; a representative of each cell is shown on the right-hand side. Bar, 10 μm.

Published March 22, 1999

were stained with DAPI, calcofluor and rhodamine-conjugated phalloidin. In tadpole cells, cortical F-actin localized exclusively in the swollen tips (Fig. 4 a, middle). Calcofluor-staining showed a huge accumulation of cell wall material in the swollen parts of the tadpole cells (Fig. 4 b, arrow). Time-lapse microscopy was performed after gene induction in order to follow morphological changes leading to the tadpole phenotype. Either the new or old end became swollen (the new end is the end that is produced after cytokinesis; the old end is the one that has already existed in the previous cycle). In Fig. 4 c, asymmetrical cell swelling that took place in the new end (marked with arrows) is shown. This analysis suggested that overproduction of Mok1 inhibited the translocation of F-actin (and cell wall materials) from one end to the other.

In contrast to the asymmetrical accumulation of actin in tadpole cells, side-by-side cells showed neither actin staining (Fig. 4 a, bottom) nor the accumulation of cell wall material (Fig. 4 b, arrowhead). These phenotypes suggest that these cells died after lysis. Nuclear staining by DAPI showed that each cell had a nucleus, indicating that chromosome segregation had been completed. In summary, the loss of Mok1 protein resulted in randomization of F-actin, whereas its overproduction abrogated translocation of F-actin from one end of the cell to the other as well as an abnormal accumulation of cell wall material and the lysis of some cells after cell division.

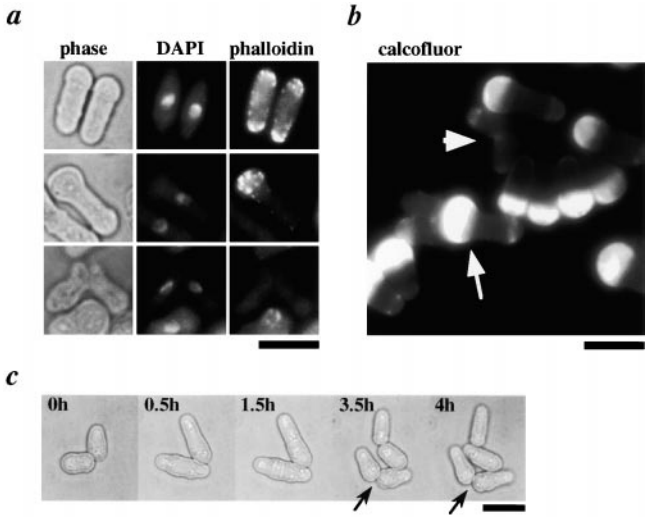

Figure 4. Overexpression of *mok1*$^+$ results in asymmetrical cell shape and abnormal accumulation of both F-actin and cell wall material. (a) Abnormal F-actin localization by *mok1*$^+$ overexpression. *mok1*$^+$-overexpressing cells were grown in the absence of thiamine for 18 h, fixed and stained with rhodamine-conjugated phalloidin (right) and DAPI (middle). Phase contrast micrographs are also shown (left). (b) Abnormal accumulation of cell wall material. *mok1*$^+$-overexpressing cells were stained with calcofluor. Tadpole cells are shown with arrow and side-by-side with arrowhead. (c) Time-lapse photography showing the production of tadpole cells. *mok1*$^+$-overexpressing cells were embedded in minimal media on a slide glass under a phase contrast microscope and photographed every 30 min. tadpole cells, in which the new end became swollen, are shown with arrows. The bar indicates 10 μm.

Mok1 Manipulation Alters the Level of α-Glucan

As Mok1 contains two separate regions that display homology to amylase and glucan synthase respectively, we were interested in measuring the level of cell wall components in mutants in which the activity of Mok1 was either down- or upregulated. For this purpose, the level of glucan in cell walls was measured through the incorporation of radioactive glucose in either ts *mok1* mutants or cells in which *mok1*$^+$ was overexpressed. As shown in Fig. 5 and Table IV, the level of glucan was significantly altered by manipulation of Mok1. Most remarkably, α-glucan levels in Mok1-overproducing cells were elevated more than threefold over compared with wild-type cells (344%). The level of galactomannan also showed a modest increase (202%), whereas the level of β-glucan decreased slightly (75%).

On the other hand, incubation of ts *mok1* mutants at the restrictive temperature resulted in a decrease in α-glucan level by 69%. In contrast, galactomannan and β-glucan levels were virtually unchanged. These results strongly suggested that Mok1 is an α-glucan synthase.

Identification of the Mok1 Protein in the Membranous Fraction

Polyclonal anti-Mok1 antibodies were prepared in order to characterize the Mok1 protein (Materials and Methods). These antibodies detected a band ~280 kD after immunoblotting of total cell extracts from wild-type cells (Fig. 6 a, lane 1). The intensity of this band increased in cells containing the *mok1*$^+$ gene on a multicopy plasmid (lane 2) and further dramatically increased in a strain in which *mok1*$^+$ was overexpressed by induction of the *nmt1* promoter (lane 3). These data showed that the antibody specifically recognized the *mok1*$^+$ gene product.

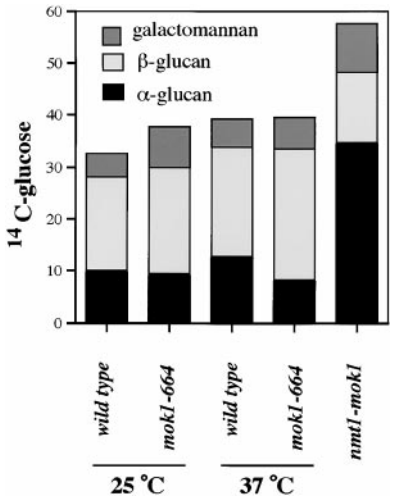

Figure 5. The level of glucan in various *mok1* mutants. The relative levels of [^{14}C]glucose radioactivity incorporated into each glucan (black, α-glucan; lightly shaded, β-glucan; densely shaded, galactomannan) are shown for each strain (wild-type, HM123; *mok1-664*, DH664; *nmt-mok1*, SKP103). Values are the means arising from at least three independent experiments (samples in duplicate). Each strain was grown at 25 or 37°C for 6 h. The exact values and the standard deviations are shown in Table IV.

Published March 22, 1999

Table IV. Incorporation of Radioactivity from [^{14}C]Glucose into Cell Wall Polysaccharide

Strain	°C	Cell wall	Galactomannan	α-Glucan	β-Glucan
Wild-type	25	32.7 ± 3.2	4.5 ± 1.4	10.1 ± 1.8	18.1 ± 2.8
Wild-type	37	39.2 ± 2.0	5.5 ± 1.9	12.7 ± 1.9	21.0 ± 2.0
mok1-664	25	37.6 ± 2.7	7.6 ± 2.6	9.4 ± 0.8	20.6 ± 0.8
mok1-664	37	39.4 ± 1.7	6.0 ± 0.6	8.3 ± 1.3	25.1 ± 3.4
nmt-mok1$^+$	25	57.4 ± 5.7	9.1 ± 1.0	34.7 ± 3.5	13.6 ± 0.2
Wild-type	30	29.0 ± 0.8	3.1 ± 0.2	9.1 ± 0.6	16.9 ± 0.3
Δpck2	30	26.3 ± 0.8	2.3 ± 0.7	6.9 ± 0.2	15.6 ± 3.1
Δpck2 nmt-mok1$^+$	30	36.0 ± 0.8	5.5 ± 0.3	18.6 ± 0.8	11.9 ± 0.9

Percent incorporation of [^{14}C]glucose incorporated per fraction/total cpm incorporated is shown. Values are the means and standard deviations calculated from three independent experiments.

Total cell extracts were fractionated and immunoblotted using anti-Mok1 antibody. Mok1 was insoluble when a low salt buffer was used for the preparation of whole cell extracts (30 mM NaCl, Fig. 6 b, lanes 1–3) or when the buffer contained high salt (0.5 M, lanes 4 and 5). Treatment with a nonionic detergent solubilized ~50% of Mok1 (lanes 6 and 7) and ionic detergent resulted in complete solubilization (lanes 8 and 9). Protein denaturation with 8 M urea also solubilized Mok1 (lanes 10 and 11). Next the half-life of the Mok1 protein was examined. After a short induction of the *mok1*$^+$ gene from the *nmt1* promoter in minimal medium without thiamine (derepressed), p280^{mok1} levels were followed by immunoblotting after the addition of thiamine and cycloheximide to repress promoter and protein synthesis respectively. It was found that Mok1 is a stable protein, a half-life is >120 min (Fig. 6 c). These results suggested that Mok1 is an stable integral membrane protein, which is consistent with the presence of several transmembrane domains (Fig. 2 a).

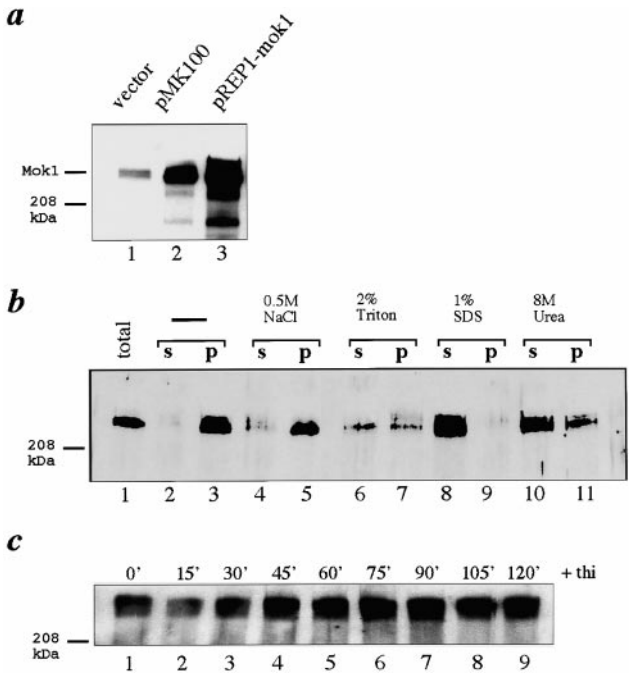

Figure 6. The Mok1 protein is stable and partitioned to the membrane fraction. (a) Identification of the Mok1 protein. Total cell extracts (20 μg) prepared from wild-type cells containing a vector (lane 1), a plasmid containing the genomic *mok1*$^+$ gene (pMK100, lane 2) or that containing *nmt-mok1*$^+$ (pREP-mok1, derepressed, lane 3) were run on 7.5% SDS-PAGE and immunoblotted with affinity-purified anti-Mok1 antibody. (b) Subcellular fractionation of the Mok1 protein. Total cell extracts were prepared from wild-type cells (lane 1) and fractionated in a buffer containing low salt (lanes 2 and 3), high salt (0.5 M NaCl, lanes 4 and 5), nonionic detergent (Triton X-100, lanes 6 and 7), ionic detergent (1% SDS, lanes 8 and 9) or denaturing reagent (8 M urea, lanes 10 and 11). s stands for the supernatant and p for the pellet. (c) Stability of Mok1. Cells that contain *mok1*$^+$ under thiamine-repressible *nmt1* promoter (SKP103) were grown to mid-log phase at 29°C in minimal medium containing 5 μg/ml thiamine, filtered, resuspended in minimal medium lacking thiamine, and incubated for 12 h. Thiamine (5 μg/ml) and cycloheximide (100 μg/ml) were then added to repress the *nmt1* promoter and protein synthesis respectively. Cell extracts were prepared every 15 min, and immunoblotting performed.

Mok1 Protein Localizes to Growing Cell Tips and Contractile Ring-like Structures

Immunofluorescence microscopy was performed using anti-Mok1 in order to determine the subcellular localization of Mok1. As shown in Fig. 7 a, Mok1 mainly localizes in two regions, cell tips and the medial region. This localization of Mok1 is very similar to that for F-actin (Marks et al., 1986; Jochová et al., 1991).

Next, cells were simultaneously double stained with anti-Mok1 and anti-actin antibodies. Anti-Mok1 antibodies stained the region of the cell that overlapped with, but not identical to, actin staining (Fig. 7 b). In a newly born small cell (Fig. 7 a, <10 μm), just after cytokinesis, Mok1 and actin localized still in the new end in which the septum had previously been formed. Then these two proteins moved to the old end (Fig. 7 b). Upon NETO (Fig. 7 c, new end take off; Mitchison and Nurse, 1985), both actin and Mok1 were seen at the new end and these two proteins existed hereafter at both ends. It is of note that, while actin mostly localized as a patched pattern, Mok1 localization at the tips was much more homogeneous and produced a uniform staining pattern (Fig. 7, b and c). At mitosis, actin and Mok1 disappeared from cell tips, and upon entry into anaphase (Fig. 7, d and e), both proteins localized in the medial region of the cell as ring-like structures, where septa would subsequently form. Finally in septating cells (Fig. 7 f), actin and Mok1 colocalized with septa and during septation (g), Mok1 staining broadened and looked as if it was doubled in width. In contrast, actin also now looked duplicated but the staining was less uniform and patched structures were more obvious. Finally, just before cell separation (Fig. 7 h), Mok1 localized as dense dot that was bounded by two sets of actin patches in the center of the two dividing cells. It should be noted that localization to dense dot upon cytokinesis has been observed in several actin binding proteins such as Cdc8 (tropomyosin; Balasuramanian et al., 1992) and Myo2 (Type II myosin; Kitayama et al., 1997). In summary Mok1 closely localizes with actin, at the growing cell tips in interphase, the medial regions in mitosis and a central dense dot during the final stage of septation.

Published March 22, 1999

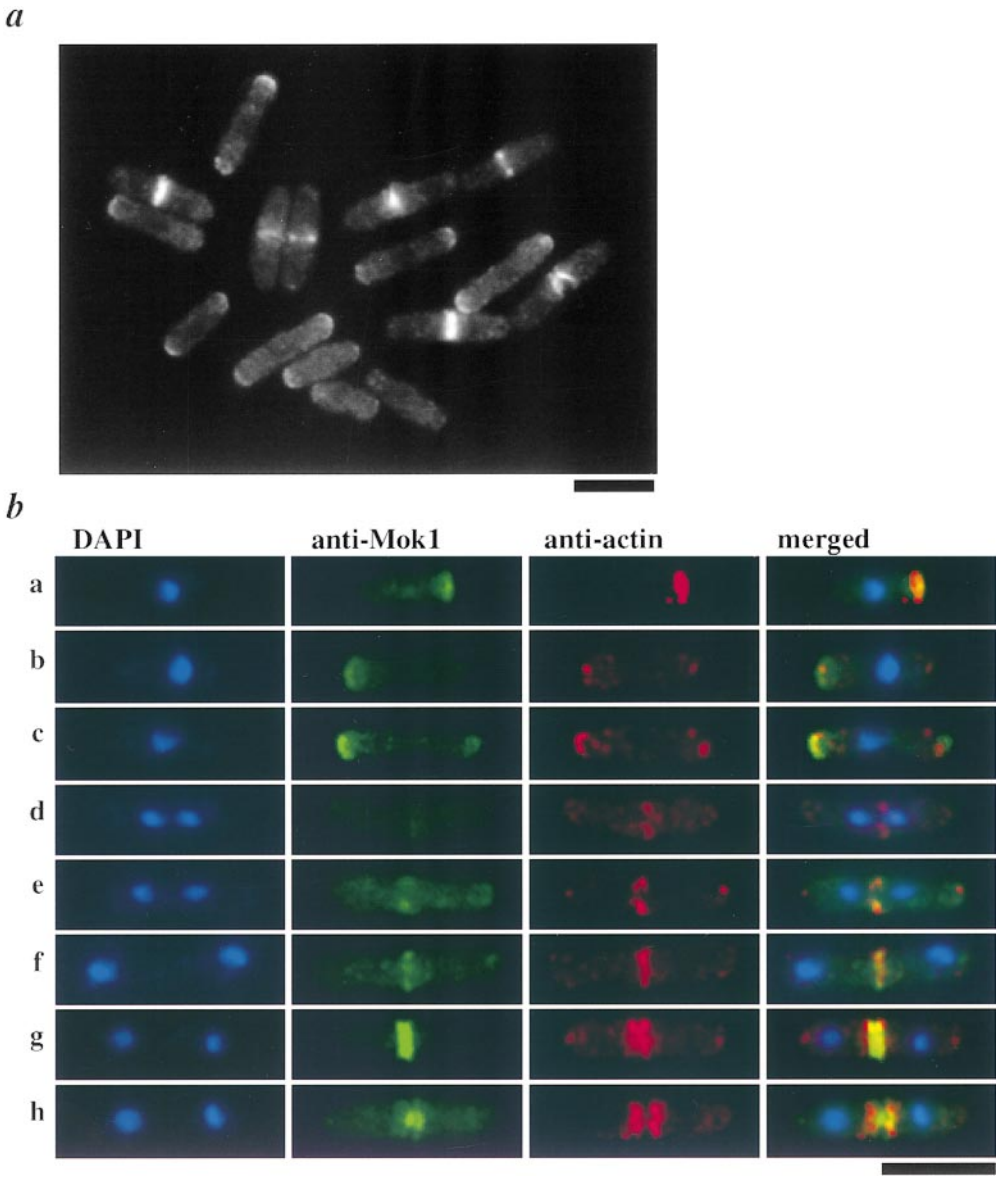

Figure 7. The Mok1 protein localizes in close proximity to the F-actin cytoskeleton. (a) Immunofluorescence microscopy using anti-Mok1 antibody. Exponentially growing wild-type cells were fixed and processed for immunofluorescence microscopy using affinity-purified anti-Mok1 antibody. (b) Double immunofluorescence microscopy using anti-Mok1 and anti-actin. Chromosomal DNA was stained with DAPI and merged images are shown in the right row. Representative patterns during each cell cycle stage are shown. Bar, 10 μm.

F-Actin Cytoskeleton Is Essential for the Specific Localization of Mok1

Given the localization of actin and Mok1 to the similar regions of the cell, we were keen to determine whether the actin cytoskeleton was required for the localization of Mok1. To address this question, F-actin was depolymerized with latrunculin A (lat A; Spector et al., 1989; Ayscough et al., 1997), and the consequence for the cellular localization of Mok1 determined. As shown in Fig. 8 a, after 10 min upon lat A addition (middle), Mok1 localization to both the growing ends and the medial regions was abolished. Immunoblotting showed that the total level of Mok1 unchanged during lat A treatment (Fig. 8 b). These results suggested that cortical actin is essential for the correct localization of Mok1.

To disrupt the actin cytoskeleton by another approach, the ts profilin mutant *cdc3* and the ts tropomyosin mutant *cdc8* (Balasubramanian et al., 1992, 1994) were incubated at the restrictive temperature to disassociate F-actin patches from the cell tips and medial regions. Under these conditions, the F-actin patches associated with the cell periphery and the actomyosin ring structure failed to form, resulting in mitosis without cytokinesis and the accumulation of multi-nucleated cells (Fig. 8 c, top and bottom). Mok1, as in lat A–treated cells, dislocalized completely in these cells (middle). We conclude that the cellular localization of Mok1 is dependent on the integrity of the F-actin cytoskeleton.

The Mok1 Protein Is Mislocalized in the mok1 Mutants

The localization of Mok1 was examined in the ts *mok1* mutants. As shown in Fig. 9 a, the Mok1 protein was no longer localized to discrete regions of the cell, instead the whole cytoplasm was stained. It should be noted that the presence of patch-like actin dots indicated that actin polymers attached with the plasma membrane as in wild-type

Published March 22, 1999

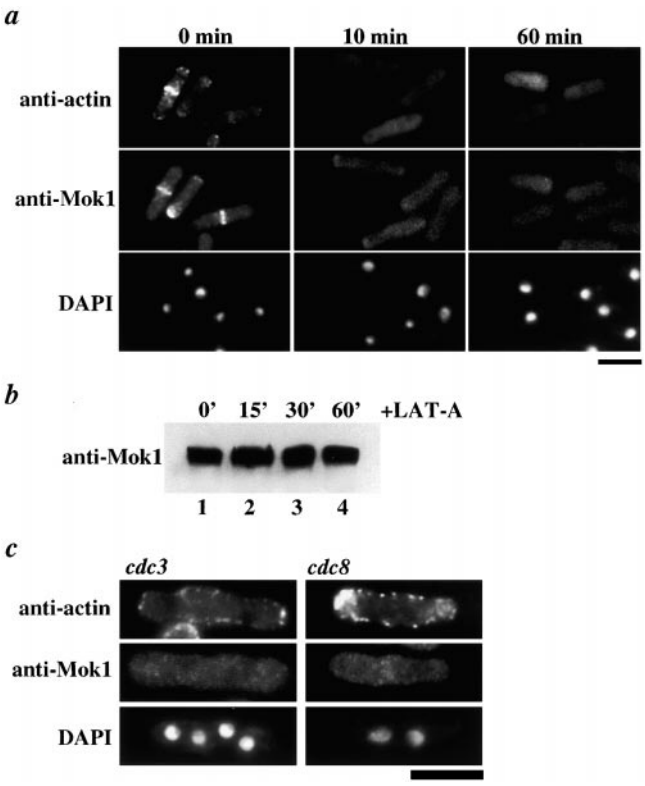

Figure 8. Mok1 localization is dependent upon the integrity of the F-actin cytoskeleton. (a) Loss of the Mok1 localization upon disruption of the F-actin cytoskeleton. Wild-type cells were treated with lat A for 1 h, and processed for immunofluorescence microscopy to localize actin (top) and Mok1 (middle), or stained with DAPI (bottom). (b) The level of Mok1 upon lat A treatment. Cell extracts were prepared at 15 min intervals after addition of lat A and immunoblotting performed with anti-Mok1 antibody. (c) Lack of the Mok1 localization to specific sites in the mutants with defects in actin-binding proteins. *cdc3-6* and *cdc8-27* mutant cells (PN18 and PN100) were grown at 35.5°C for 6 h, processed for immunofluorescence microscopy. Bar, 10 μm.

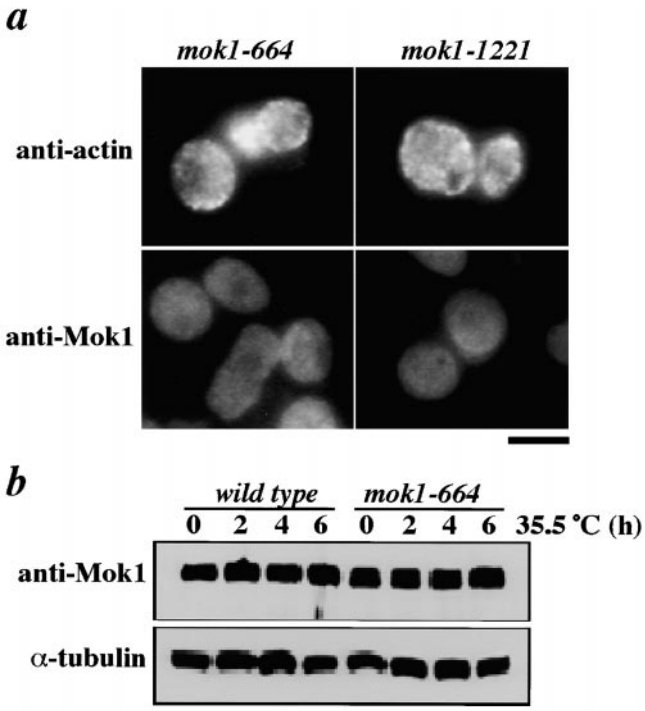

Figure 9. Mok1 distribution is disrupted in ts *mok1* mutants. (a) Defective Mok1 localization in ts *mok1* mutants. *mok1-664* and *-1221* mutant cells were grown at 35.5°C for 6 h, fixed and stained with anti-actin (upper) or anti-Mok1 antibody (lower). Bar, 10 μm. (b) Mok1 protein levels in ts *mok1* mutants. Wild-type or *mok1-664* mutant cells were grown at 35.5°C for 6 h and aliquots were collected at 2-h intervals. Cell extracts (20 μg) were prepared, run on 7.5% SDS-PAGE and immunoblotted with anti-Mok1 antibody (upper) or with anti–α-tubulin antibody (lower).

cells in *mok1* mutant cells (Mulholland et al., 1994). This mislocalized pattern of Mok1 was reminiscent of that in cells in which the actin cytoskeleton had been disrupted (Fig. 8). The level of the Mok1 protein was indistinguishable between wild-type and ts *mok1* mutants grown at the restrictive temperature (Fig. 9 b), indicating that the apparent lack of the specific localization of Mok1 was not due to reduced protein levels. These results suggested that Mok1 localization requires intact Mok1 activity and/or structure and that the ts Mok1 proteins fail to be transported to the plasma membrane, which leads to randomization of F-actin and cell shape defects.

Mok1 Localization Is Dependent on Pck2 and both Proteins Coordinately Regulate Cell Wall Integrity

We sought to examine the functional relationship between Mok1 and Pck1/2. To this end, the cellular localization of Mok1 was examined in *pck2* mutant. It was found that Mok1 became mislocalized in this mutant (Fig. 10 a, upper left); neither the cell tips nor the medial regions were stained with anti-Mok1 antibody, instead a dispersed pattern was observed. Immunoblotting showed that the amount of Mok1 did not alter between wild-type and *pck2* mutant (lower). In contrast the localization of F-actin appeared not to be severely impaired as cortical actin existed at either the cell tips or the medial regions (upper right).

Next the double mutants between ts *mok1* and Δ*pck2* were constructed. *mok1-664*Δ*pck2* was synthetically lethal at 30°C, a temperature at which either single mutant could grew (Fig. 10 b). Synthetic lethality was not observed between *mok1-664* and Δ*pck1*, consistent with our previous result showing that $pck2^+$ plays the major role (Toda et al., 1993). Although *mok1-664*Δ*pck2* managed to form colonies at 27°C, double mutant cells were round and spontaneously lysed (Fig. 10 c), suggesting that cell wall integrity was substantially impaired. This was confirmed by glucanase treatment of the double mutants grown at 27°C, as this strain was lysed much faster than either wild-type or each single mutant alone (Fig. 10 d). These data indicate that Pck2 is required for the specific localization of Mok1 and that Mok1 regulates cell wall integrity either in parallel with or downstream of Pck1/2.

Mok1 Acts Downstream of Protein Kinase C–related Pck1 and Pck2

To distinguish between the possibilities that Mok1 acts in parallel with or downstream of the Pck1 and Pck2 path-

Published March 22, 1999

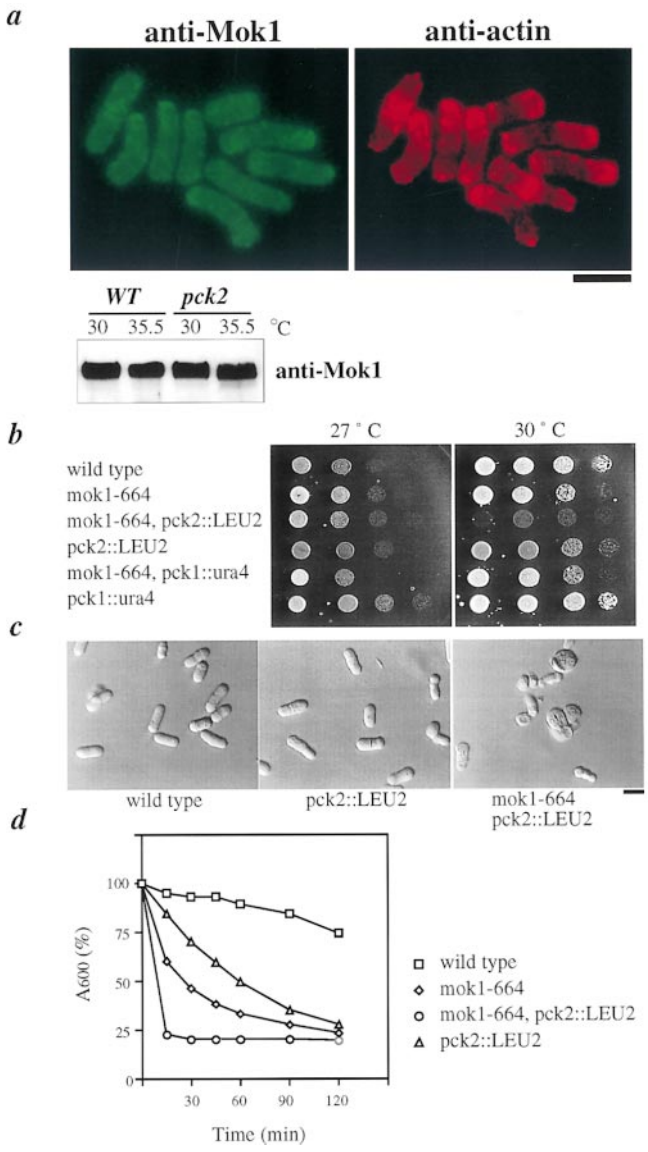

Figure 10. Pck2 is required for Mok1 localization and the mutations in both genes are synthetically lethal. (a) Mok1 localization in *pck2* mutant. *pck2* mutant cells were grown at 35.5°C for 4 h and processed for immunofluorescence microscopy using anti-Mok1 (upper left) and anti-actin antibodies (upper right). The amount of Mok1 in wild-type and *pck2* mutant is also shown (lower). (b) Synthetic lethal interaction between ts *mok1* and Δ*pck2* at 30°C. Various strains (wild-type, HM123; *mok1-664*, DH664; *mok1-664*Δ*pck2*, SKP100; Δ*pck2*, TP170-2B; *mok1-664*Δ*pck1*, SKP101; and Δ*pck1*, TP134-3B) were spotted onto rich YPD plates as serial dilutions (10^6 cells in the left row and then diluted 10-fold in each subsequent spot on the right) and incubated at 27°C (the left plate) or 30°C (right). (c) The round cell morphology of the *mok1-664*Δ*pck2* mutants. Cell morphology of exponentially growing wild-type (left), Δ*pck2* (middle), or *mok1-664*Δ*pck2* (right) cells at 27°C is shown. The bar indicates 10 μm. (d) Defects in cell wall integrity in the *mok1-664*Δ*pck2* mutants. Each strain was treated with β-glucanase (50 μg/ml) at 27°C.

way, the *nmt1-mok1*$^+$ gene was overexpressed in Δ*pck2* cells (chromosomally integrated, SKP170). If Mok1 is somehow regulated by Pck1 and Pck2, Δ*pck2* cells should become resistant to simple overexpression of *mok1*$^+$ as Mok1 activity is expected to be compromised in the absence of Pck2 function. On the other hand, if Mok1 and Pck2 (and Pck1) regulate cell wall integrity in a parallel manner, *nmt1-mok1*$^+$ should be as toxic in Δ*pck2* cells as in wild-type cells or it might even be more toxic. As shown in Fig. 11 a, Δ*pck2* cells became insensitive to *nmt1-mok1*$^+$, they were capable of forming colonies in the derepressed conditions, whereas wild-type cells were not. Consistent with this, calcofluor staining showed that morphology of cells in which *mok1*$^+$ was overexpressed was less abnormal in Δ*pck2* than in wild-type; neither tadpole cells nor asymmetrical accumulation of cell wall materials were observed (Fig. 11 b). The lack of toxicity of *nmt1-mok1*$^+$ was not due to a reduction in the levels of Mok1 in the Δ*pck2* background (Fig. 11 c).

The level of cell wall glucan was measured in Δ*pck2* mutant or that containing *nmt1-mok1*$^+$. α-glucan level was decreased in Δ*pck2* mutant (24% reduction, Fig. 11 d and Table IV). The level of α-glucan in Δ*pck2* cells containing *nmt1-mok1*$^+$ was elevated, but the increase was greatly compromised compared with a wild-type strain containing *nmt1-mok1* (46% lower). The reduced level of α-glucan together with mislocalization of Mok1 might explain why Δ*pck2* mutant is tolerant to Mok1 overproduction. Taken together, the data suggested that Mok1 acts downstream, either directly or indirectly, of Pck1 and Pck2.

Discussion

mok1$^+$ *Encodes an Essential Fission Yeast α-Glucan Synthase*

Three lines of evidence indicate that Mok1 is a fission yeast α-glucan synthase. The amino acid sequence of Mok1 shows high homology to glycogen or starch synthase, and contains the consensus sequence for UDP-glucose binding. UDP-glucose is used as a substrate for glucan synthase. Second, overexpression of *mok1*$^+$ results in 3.5-fold increase, while mutation of the gene results in a 30% reduction in the amount of α-glucan. Third, no homologous proteins exist in budding yeast, whose cell wall lacks the α-glucan (Cabib et al., 1997). During the preparation of this manuscript, we learned that Hochstenbach et al. (1998) have also isolated *mok1*$^+$, and concluded that it encodes an α-glucan synthase (the gene was designated *ags1*$^+$).

The Cellular Localization of Mok1

The cell cycle–dependent targeting of Mok1 to the growing tips, the medial region and contractile ring-like structures is consistent with the identification of Mok1 as α-glucan synthase. These regions correspond to the sites at which cell surface structures are being actively remodeled, and both synthesis and degradation of the cell wall glucan take place to ensure tip growth, septum formation and cell separation respectively. We propose that in fission yeast 1,3-β-D-glucan synthase and glucanases also colocalize at these sites. Previous and ongoing work has suggested that Rho1 (Arellano et al., 1997; Nakano et al., 1997) and Pck1 and Pck2 (Sayers, L., K. Nakano, I. Mabuchi, S. Katayama, T. Toda, and P. Parker, unpublished results) are intimately associated with the actin cytoskeleton. It is in-

Published March 22, 1999

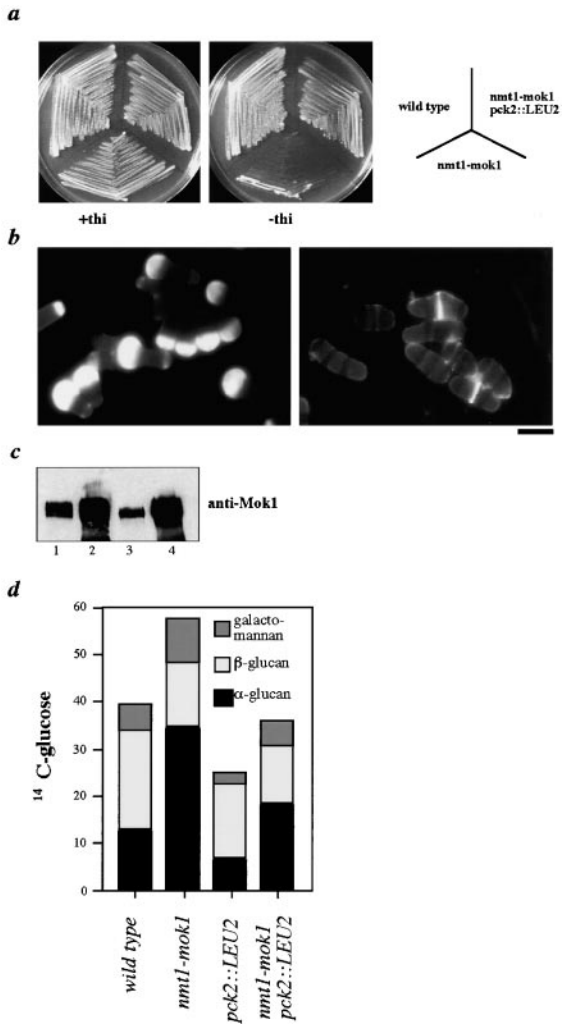

Figure 11. *pck2* mutants are insensitive to *mok1*$^+$ overexpression and lowered in α-glucan level. (a) Tolerance of Δ*pck2* to *mok1*$^+$ overexpression. Wild-type or Δ*pck2* cells in which *nmt-mok1*$^+$ was integrated into the genome (SKP103 and SKP170, respectively) were streaked on minimal medium (supplemented with leucine) in the presence (left, repressed) or absence (middle, derepressed) of thiamine, and incubated at 29°C for 3 d. (b) Cell morphology of Δ*pck2* cells upon *mok1*$^+$ overexpression. The above two strains (SKP103, left; SKP170, right) were grown in liquid minimal medium (supplemented with leucine) for 16 h and cells stained with calcofluor. The bar indicates 10 μm. (c) The level of the Mok1 protein. The two strains (SKP103, lanes 1 and 2; SKP170, lanes 3 and 4) were grown in the liquid minimal in the absence of thiamine. Total cell extracts (5 μg) were prepared at time 0 (lanes 1 and 3) and 16 h later (lanes 2 and 4), and immunoblotting performed. (d) The level of glucan in Δ*pck2* mutant. Relative amount of [^{14}C]glucose radioactivity incorporated into each glucan was measured as in Fig. 5. Wild-type (HM123), Δ*pck2* (TP170-2B) and Δ*pck2* containing *nmt-mok1*$^+$ (SKP170) were grown at 30°C. The value of wild-type containing *nmt-mok1*$^+$ (SKP103, Fig. 5) is shown as a comparison. The exact values and the standard deviations are shown in Table IV.

triguing that all the proteins that constitute a sequential effector pathway (Rho1-Pck1/2-Mok1) appear to colocalize. The molecular mechanisms underlying the integration of these multiple enzymatic systems at these sites remain to be addressed.

What is the molecular basis of Mok1 association with the plasma membrane? The presence of a putative signal peptide in the NH_2 terminus suggests that Mok1 is first translocated into the endoplasmic reticulum via the secretory pathway. It would be logical to suppose that this transport is followed by translocation into the plasma membrane through the Golgi and vesicle fusion (Kaiser et al., 1997). The dependency of Mok1 localization upon the integrity of the F-actin cytoskeleton is consistent with this idea. Recent analysis shows that polarized delivery of secretory vesicles requires actin cables rather than cortical actin (Pruyne et al., 1998) and Mok1 localization may be also dependent on actin cables. Then why would F-actin be required to maintain Mok1 localization? The total level of Mok1 remained unchanged upon F-actin disruption, suggesting that it is unlikely that protein instability leads to the loss of specific localization of Mok1. It is possible that Mok1 turns over rapidly at the cell tips or medial regions and that, in the absence of F-actin integrity, it accumulates at some stage of the secretory pathway. This situation is analogous to actin, which turns over rapidly and disassembles instantly upon lat A treatment (Ayscough et al., 1997).

Mok1 as a Downstream Effector of Pck1 and Pck2

pck2 mutant shows the reduced level of cell wall α-glucan and is resistant to toxic overproduction of Mok1. This suggests that Pck2 positively regulates Mok1 activity. In addition, Pck2 is required for Mok1 localization at the specific sites. Mok1 and Pck1/2 do not interact in yeast two-hybrid methods (Katayama, S., and T. Toda, unpublished results). It is possible that Pck2 regulates Mok1 indirectly via some regulators. Alternatively Mok1 may be a direct substrate of Pck2 such that Pck2-dependent phosphorylation is essential for the cellular localization and enzymatic activities of Mok1. The predicted amino acid sequence of Mok1 contains thirty consensus phosphorylation sites for PKC. It might be significant that all these sites are found in the domain that shows a homology to glycogen synthase.

Although we have shown that Mok1 could be a downstream target of Pck1 and Pck2, it may not be the sole molecule by which Pck1 and Pck2 regulate cell morphology. In sharp contrast to the resistance of *pck2* mutants to Mok1 overproduction, overproduction of Pck2 is as toxic in the ts *mok1* mutants as in wild-type (Toda et al., 1993; Katayama, S., and T. Toda, unpublished results). This suggests that Pck1 and Pck2 regulate cell wall integrity via some effectors in addition to Mok1. Candidates include β-glucan metabolic enzymes, synthases or glucanases. Thus, in cells in which *pck2*$^+$ is overexpressed, the level of β- as well as α-glucan increases (Arellano, M., and P. Pérez, unpublished results). It is highly possible that Pck1 and Pck2 regulate both α-glucan and β-glucan levels to ensure a coordinated regulation of the levels of these two major cell wall components.

Structural Determinants for the Membrane-bound Mok1 Localization

The Mok1 protein consists of several putative transmembrane domains, three of which lie in the NH_2-terminal amylase-homologous domains, one in the central region of the protein and twelve at the COOH terminus. Consistent

Published March 22, 1999

with this, the protein behaved as a membrane-bound protein. COOH-terminal tagging by fusion with DNA sequences encoding either HA-peptide or GFP completely abolishes Mok1 function. We suspect that tagging blocks the correct localization of Mok1 by disrupting the function of the membrane-spanning domains.

In this context, it is of interest that the Mok1 protein derived from a ts *mok1-664* strain also failed to localize correctly. As with the other eight ts *mok1* mutant alleles examined, the mutation site in *mok1-664* is not in the COOH terminus, but rather in the NH_2-terminal amylase-homologous domain. The precise role of this domain is unclear at present, but it may be required not only for reorganization of α-glucan via a transglycosylase activity as suggested (Hochstenbach et al., 1998) but also for the specific localization of Mok1. Multiple domains, therefore, appear to be responsible for the plasma membrane-bound localization of Mok1, and this association appears to be essential for Mok1 function.

Protein Family of Mok1

Generally genes encoding glucan synthases appear to comprise multi-gene families. In addition to five members of the Mok1 family of α-glucan synthase, the fission yeast genome contains at least three 1,3-β-D-glucan synthase homologues (Katayama, S., and T. Toda, unpublished results). In budding yeast, three 1,3-β-D-glucan synthase-encoding genes and two for 1,6-β-D-glucan synthase-encoding genes have been identified (Orlean, 1997). Furthermore there are three chitin synthase-encoding genes in budding yeast and six in *Aspergillus nidulans* (Orlean, 1997). The biological significance of five Mok1-related proteins is currently unclear as *mok1*$^+$ is by itself essential for cell viability. Simultaneous triple deletions of the other four homologues (Δ*mok11*Δ*mok12*Δ*mok14*) do not affect viability in normal media. It is possible that these homologues become important in certain growth conditions such as stress and different growth media. It would be of significant to know how these multiple α-glucan synthase homologues are functionally distinct and differentially regulated during mitotic and meiotic cycles.

We thank Drs. Hirofumi Nakano for staurosporine and K-252a, Iain Hagan for FITC-conjugated anti–rabbit IgG secondary antibody, Paul Nurse for strains, John Sgouros for help for bioinformatics and structural predictions, and Mohan K. Balasubramanian and Yasuhisa Adachi for discussion. We are grateful to Dr. Frans Hochstenbach for exchanging data. We thank Drs. Iain Hagan, Paul Nurse, and Peter J. Parker for careful reading of the manuscript and useful suggestions.

The initial part of this work was supported by a grant from Kyowa Hakko Co. Ltd.

Received for publication 15 October 1998 and in revised form 4 February 1999.

References

Amano, M., H. Mukai, Y. Ono, K. Chihara, T. Matsui, Y. Hamajima, K. Okawa, A. Iwamatsu, and K. Kaibuchi. 1996. Identification of a putative target for Rho as the serine-threonine kinase protein kinase N. *Science.* 271: 648–650.

Arellano, M., A. Durán, and P. Pérez. 1996. Rho1 GTPase activates the (1-3)β-D-glucan synthase and is involved in *Schizosaccharomyces pombe* morphogenesis. *EMBO (Eur. Mol. Biol. Organ.) J.* 15:4584–4591.

Arellano, M., A. Duran, and P. Pérez. 1997. Localisation of the *Schizosaccharomyces pombe* rho1p GTPase and its involvement in the organisation of the actin cytoskeleton. *J. Cell Sci.* 110:2547–2555.

Ayscough, K.R., J. Stryker, N. Pokala, M. Sanders, P. Crews, and D.G. Drubin. 1997. High rates of actin filament turnover in budding yeast and roles for actin in establishment and maintenance of cell polarity revealed using the actin inhibitor latrunculin-A. *J. Cell Biol.* 137:399–416.

Bähler, J., J. Wu, M.S. Longtine, N.G. Shah, A. McKenzie III, A.B. Steever, A. Wach, P. Philippsen, and J.R. Pringle. 1998. Heterologous modules for efficient and versatile PCR-based gene targeting in *Schizosaccharomyces pombe. Yeast.* 14:943–951.

Balasubramanian, M.K., D.M. Helfman, and S.M. Hemmingsen. 1992. A new tropomyosin essential for cytokinesis in the fission yeast *S. pombe. Nature.* 360:84–87.

Balasubramanian, M.K., B.R. Hirani, J.D. Burke, and K.L. Gould. 1994. The *Schizosaccharomyces pombe cdc3*$^+$ gene encodes a profilin essential for cytokinesis. *J. Cell Biol.* 125:1289–1301.

Cabib, E., T. Drgon, J. Drgonová, R.A. Ford, and R. Kollár. 1997. The yeast cell wall, a dynamic structure engaged in growth and morphogenesis. *Biochem. Soc. Trans.* 1:200–204.

Drgonová, J., T. Drgon, K. Tanaka, R. Kollár, G.-C. Chen, R.A. Ford, C.S.M. Chan, Y. Takai, and E. Cabib. 1996. Rho1p, a yeast protein at the interface between cell polarization and morphogenesis. *Science.* 272:277–279.

Drubin, D.G., and W.J. Nelson. 1996. Origins of cell polarity. *Cell.* 84:335–344.

Flynn, P., H. Mellor, R. Palmer, G. Panayotou, and P.J. Parker. 1998. Multiple interactions of PRK1 with RhoA. functional assignment of the HR1 motif. *J. Biol. Chem.* 273:2698–2705.

Furukawa, K., M. Tagaya, K. Tanizawa, and T. Fukui. 1993. Role of the conserved Lys-X-Gly-Gly sequence at the ADP-glucose-binding site in *Escherichia coli* glycogen synthase. *J. Biol. Chem.* 268:23837–23842.

Hall, A. 1998. Rho GTPases and the actin cytoskeleton. *Science.* 279:509–514.

Henrissat, B., and G. Davies. 1997. Structural and sequence-based classification of glycoside hydrolases. *Curr. Opin. Struct. Biol.* 7:637–644.

Hochstenbach, F., F.M. Klis, H. van den Ende, E. van Donselaar, P.J. Peters, and R.D. Klausner. 1998. Identification of a putative alpha-glucan synthase essential for cell wall construction and morphogenesis in fission yeast. *Proc. Natl. Acad. Sci. USA.* 95:9161–9166.

Ishiguro, J. 1998. Genetic control of fission yeast cell wall synthesis: the genes involved in wall biogenesis and their interactions in *Schizosaccharomyces pombe. Genes Genet. Syst.* 73:181–191.

Ishiguro, J., A. Saitou, A. Durán, and J.C. Ribas. 1997. *cps1*$^+$, a *Schizosaccharomyces pombe* gene homolog of *Saccharomyces cerevisiae FKS* genes whose mutation confers hypersensitivity to cyclosporin A and papulocandin B. *J. Bacteriol.* 179:7653–7662.

Jochová, J., I. Rupes, and E. Streiblová. 1991. F-actin contractile rings in protoplasts of the yeast *Schizosaccharomyces pombe. Cell Biol. Int. Rep.* 15:607–610.

Kaiser, C.A., R.E. Gimeno, and D.A. Shaywitz. 1997. Protein secretion, membrane biogenesis, and endocytosis. *In* The Molecular and Cellular Biology of the Yeast *Saccharomyces.* Vol. 3. J.R. Pringle, J.R. Broach, and E.W. Jones, editors. Cold Spring Harbor Laboratory Press, Cold Spring Harbor, NY. 91–227.

Kitayama, C., A. Sugimoto, and M. Yamamoto. 1997. Type II myosin heavy chain encoded by the *myo2* gene composes the contractile ring during cytokinesis in *Schizosaccharomyces pombe. J. Cell Biol.* 137:1309–1319.

Kobori, H., T. Toda, H. Yaguchi, M. Toya, M. Yanagida, and M. Osumi. 1994. Fission yeast protein kinase C homologues are required for protoplast regeneration: a functional link between cell wall formation and cell shape control. *J. Cell Sci.* 107:1131–1136.

Kopecká, M., G.H. Fleet, and H.J. Phaff. 1995. Ultrastructure of the cell wall of *Schizosaccharomyces pombe* following treatment with various glucanases. *J. Struct. Biol.* 114:140–152.

Kumar, A., C.E. Larsen, and J. Preiss. 1986. Biosynthesis of bacterial glycogen. primary structure of *Escherichia coli* ADP-glucose: alpha-1,4-glucan, 4-glucosyltransferase as deduced from the nucleotide sequence of the *glgA* gene. *J. Biol. Chem.* 261:16256–16259.

Kyte, J., and R.F. Doolittle. 1982. A simple method for displaying the hydropathic character of a protein. *J. Mol. Biol.* 157:105–132.

Levin, D.E., and E. Bartrett-Heubusch. 1992. Mutants in the *S. cerevisiae PKC1* gene display a cell cycle-specific osmotic stability defect. *J. Cell Biol.* 116: 1079–1088.

Manners, D.J., and M.T. Meyer. 1977. The molecular structure of some glucans from the cell wall of *Schizosaccharomyces pombe. Carbohydr. Res.* 57:189–203.

Marks, M., and J.S. Hyams. 1985. Localization of F-actin through the cell division cycle of *Schizosaccharomyces pombe. Eur. J. Cell Biol.* 39:27–32.

Marks, J., I.M. Hagan, and J.S. Hyams. 1986. Growth polarity and cytokinesis in fission yeast: the role of the cytoskeleton. *J. Cell Sci. Suppl.* 5:229–241.

Maundrell, K. 1990. *nmt1* of fission yeast. *J. Biol. Chem.* 265:10857–10864.

Mitchison, J.M., and P. Nurse. 1985. Growth in cell length in the fission yeast *Schizosaccharomyces pombe. J. Cell Sci.* 75:357–376.

Moreno, S., A. Klar, and P. Nurse. 1991. Molecular genetic analyses of fission yeast *Schizosaccharomyces pombe. Methods Enzymol.* 194:773–782.

Mulholland, J., D. Preuss, A. Moon, A. Wong, D. Drubin, and D. Botstein. 1994. Ultrastructure of the yeast actin cytoskeleton and its association with the plasma membrane. *J. Cell Biol.* 125:381–391.

Nakano, K., R. Arai, and I. Mabuchi. 1997. The small GTP-binding protein Rho1 is a multifunctional protein that regulates actin localization, cell polarity, and septum formation in the fission yeast *Schizosaccharomyces pombe.*

Genes Cells. 2:679–694.

Nonaka, H., K. Tanaka, H. Hirano, T. Fujiwara, H. Kohno, M. Umikawa, A. Mino, and Y. Takai. 1995. A downstream target of *RHO1* small GTP-binding protein is *PKC1*, a homolog of protein kinase C, which leads to activation of the MAP kinase cascade in *Saccharomyces cerevisiae*. *EMBO (Eur. Mol. Biol. Organ.) J.* 14:5931–5938.

Nurse, P. 1994. Fission yeast morphogenesis-posing the problems. *Mol. Biol. Cell*. 5:613–616.

Orlean, P. 1997. Biogenesis of yeast wall and surface components. *In* The Molecular and Cellular Biology of the Yeast *Saccharomyces.* Vol. 3. J.R. Pringle, J.R. Broach, and E.W. Jones, editors. Cold Spring Harbor Laboratory Press, Cold Spring Harbor, NY. 229–362.

Pruyne, D.W., D.H. Schott, and A. Bretscher. 1998. Tropomyosin-containing actin cables direct the Myo2p-dependent polarized delivery of secretory vesicles in budding yeast. *J. Cell Biol.* 143:1931–1945.

Qadota, H., C.P. Python, S.B. Inoue, M. Arisawa, Y. Anraku, Y. Zheng, T. Watanabe, D.E. Levin, and Y. Ohya. 1996. Identification of yeast Rho1p GTP–ase as a regulatory subunit of 1,3-β-glucan synthetase. *Science.* 272:279–281.

Ridley, A.J. 1996. Rho: theme and variations. *Curr. Biol.* 6:1256–1264.

Sambrook, J., E.F. Fritsch, and T. Maniatis. 1989. Molecular Cloning: A Laboratory Manual. Cold Spring Harbor Laboratory Press, Cold Spring Harbor, NY. 545 pp.

Sanger, F., S. Nicklen, and A.R. Coulson. 1977. DNA sequencing with chain-terminating inhibitors. *Proc. Natl. Acad. Sci. USA*. 74:5463–5467.

Shiozaki, K., and P. Russell. 1995. Counteractive roles of protein phosphatase 2C. (PP2C) and a MAP kinase kinase homolog in the osmoregulation of fission yeast. *EMBO (Eur. Mol. Biol. Organ.) J.* 14:492–502.

Spector, I., N. Shochet, D. Blasberger, and Y. Karshaman. 1989. Latrunculins-novel marine macrilides that disrupt microfilament organization and affect cell growth: 1. comparison with cytochalasin D. *Cell Motil. Cytoskeleton*. 13: 127–144.

Tamaoki, T., and H. Nakano. 1990. Potent and specific inhibitors of protein kinase C of microbial origin. *Biotechnol.* 8:732–735.

Tanaka, K., and K. Takai. 1998. Control of reorganization of the actin cytoskeleton by Rho family GTP-binding proteins in yeast. *Curr. Opin. Cell Biol.* 10: 112–116.

Toda, T. 1997. Genetic approaches in yeast. *In* Protein kinase C. Molecular Biology Intelligence Unit. P.J. Parker, and L.V. Dekker, editors. R.G. Landes Company, Georgetown, TX. 189–203.

Toda, T., M. Shimanuki, and M. Yanagida. 1993. Two novel protein kinase C-related genes of fission yeast are essential for cell viability and implicated in cell shape control. *EMBO (Eur. Mol. Biol. Organ.) J.* 12:1987–1995.

Toda, T., S. Dhut, G. Superti-Furga, Y. Gotoh, E. Nishida, R. Sugiura, and T. Kuno. 1996a. The fission yeast *pmk1*$^{+}$ gene encodes a novel MAPK homologue which regulates cell integrity and functions coordinately with the PKC pathway. *Mol. Cell. Biol.* 16:6752–6764.

Toda, T., H. Niwa, T. Nemoto, S. Dhut, M. Eddison, M. Yanagida, and D. Hirata. 1996b. Fission yeast *sts5*$^{+}$ is required for establishment of growth polarity and functionally interacts with protein kinase C and an osmosensing MAP-kinase pathway. *J. Cell Sci.* 109:2331–2342.

van der Leij, F.R., R.G. Visser, A.S. Ponstein, E. Jacobsen, and W.J. Feenstra. 1991. Sequence of the structural gene for granule-bound starch synthase of potato (*Solanum tuberosum L.*) and evidence for a single point deletion in the *amf* allele. *Mol. Gen. Genet.* 228:240–248.

Watanabe, N., Y. Saito, P. Madaule, T. Ishizaki, K. Fujisawa, N. Morii, H. Mukai, Y. Ono, A. Kakizuka, and S. Narumiya. 1996. Protein kinase N (PKN) and PKN-related protein Rhophilin as targets of small GTPase Rho. *Science*. 271:645–648.